Table III. Syntheses of Heteroarylmethyl Chlorides

compd	method[a]	ref
7	A	
8	A	
9	A	
10	B	27, 28
11	B	27, 28
12	C	29
13	C	30
14	D	31
15	C	32
16	E	33
17	D	34
18	E	35

[a] A, chlorination of commercially available carbinol; B, because of the reported explosiveness of these compounds,[27] extremely mild chlorination conditions were employed;[28] C, from corresponding carboxylic acid; D, from hydrocarbon via lithiation and carbonation to yield acid; E, direct chloromethylation of hydrocarbon.

Experimental Section

Materials. All compounds were purified before use and exhibited physical and spectroscopic properties in agreement with literature values. GLC indicated purities in excess of 99%.

Triphenyltin hydride was prepared according to the standard method of Hoyte and Denney.[26] Because of the extreme probable lability of heteroarylmethyl chlorides, these compounds were prepared just prior to use. The general, but not exclusive, means of carrying this out was by treatment of the corresponding heteroarylcarbinol by thionyl chloride. These, in turn, were frequently obtained by lithium aluminum hydride reduction of the corresponding carboxylic acids. Table III lists the methods employed to prepare each heteroarylmethyl chloride as well as pertinent references for the syntheses of starting material.

Kinetics. Solutions of two arylmethyl chlorides, internal standard (diphenylmethane or *tert*-butylbenzene), initiator (azo*bis*(isobutyronitrile)), and benzene were prepared in approximate molar ratios of 1:1:1:0.1:100 and distributed into ampules. A small amount of the mixture was reserved for analysis of the starting material. The ampules were frozen in an acetone–dry ice slurry as soon as possible. A solution of triphenyltin hydride and benzene in the approximate molar ratio of 1:12.5 was prepared and added to the above samples. The ampules were then sealed under a reduced pressure of nitrogen and were placed in a constant temperature bath maintained at 70.0 ± 0.2 °C for times varying from 1 to 4 h. After completion of the reaction, the ampules were opened and analyzed for the disappearance of the (chloromethyl)arenes and the appearance of the arylmethanes via nuclear magnetic resonance, using the aliphatic protons of diphenylmethane or *tert*-butylbenzene as internal standards. The procedure was to have the two arylmethyl chlorides compete directly for the triphenyltin radical. Benzyl chloride was the reference compound of choice. However, when one of the arylmethyl chlorides was too reactive to compare directly with benzyl chloride, or when the benzylic protons in the two compounds overlapped, the reactivity was determined relative to some other arylmethyl chloride. The value thus obtained was converted to the desired expression by using a standard equation. Treatment of data was accomplished by utilizing standard competitive kinetic formalism.[36]

Acknowledgment. We thank Ms. Susan Randall for obtaining all NMR spectra. Appreciation is also expressed to the National Science Foundation for providing the funds for purchase of the NMR equipment and to the Computer Center of Oregon State University for providing the resources for all calculations. One of us, Helene Soppe-Mbang, also expresses her deepest gratitude to the African-American Institute for their support throughout this work.

(26) Hoyte, R. M.; Denney, D. B. *J. Org. Chem.* **1974**, *39*, 2610.
(27) Gilman, H.; Vernon, C. C. *J. Am. Chem. Soc.*, **1924**, *46*, 2576.
(28) Kirmer, D. R. *J. Am. Chem. Soc.* **1928**, *50*, 1955.
(29) Fuson, R. C.; Kneisley, J. W.; Kaiser, E. W. "Organic Synthesis", Collect. Vol. 3; Wiley: New York, 1955; p 209.
(30) Martynoff, M. *Bull. Soc. Chim. Fr.* **1952**, *19*, 1056.
(31) Gilman, H.; Dietrich, J. J. *J. Am. Chem. Soc.* **1957**, *79*, 1493.
(32) Borsche, W.; Bothe, W. *Chem. Ber.* **1909**, *42*, 1940.
(33) Johnson, R. G.; Willis, H. B.; Martini, G. A.; Kirkpatric, W. H.; Swiss, J.; Gilman, H. *J. Org. Chem.* **1956**, *21*, 457.
(34) Browne, E. J. *Aust. J. Chem.* **1975**, *28*, 1803.
(35) Gilman, H.; Stuckwisch, C. G. *J. Am. Chem. Soc.* **1943**, *65*, 1461.
(36) Gleicher, G. J. *J. Org. Chem.* **1968**, *30*, 332.

Flash Photolytic Triplet Sensitization and the Mechanism of Carbonylferroporphyrin Photodissociation

Marlene A. Stanford and Brian M. Hoffman*

Contribution from the Department of Chemistry, Northwestern University, Evanston, Illinois 60201. *Received October 14, 1980*

Abstract: Triplet sensitization is used to examine the nature and energy of the electronic state(s) involved in photodissociation from a carbonylferroporphyrin and to study the sensitized production of the zinc porphyrin triplet state in parallel observations. Both processes are reversible over ordinary time scales, and thus we have employed a flash photolytic sensitization procedure in which the concentration of the "photoproduct" is measured in a time short compared to its lifetime, and the relative amounts generated by direct and sensitized excitation are assessed. Through the use of an appropriate suite of donors, we show that CO release occurs subsequent to triplet excitation transfer to a carbonylferroporphyrin state(s) with higher than singlet multiplicity and with energy no higher than 14 300 cm^{-1}, most probably $^3(\pi-\pi^*)$. These measurements suggest the possibility that CO photodissociation occurs via a relaxation process which proceeds through the lowest lying porphyrin ($\pi-\pi^*$) singlet (^1Q) and triplet (^3Q) states.

Carbon monoxide photodissociation from carboxyhemoglobin has been recognized for 85 years,[1] since it was noted that exposing a mixture of oxyhemoglobin and carbon monoxyhemoglobin to solar illumination produces a marked decrease in the amount of HbCO and an increase in HbO_2.[2] Ligand photodissociation is a general property of ferrohemes and hemoproteins and has been investigated in detail, beginning with the classical series of experiments which showed that the CO heme of myoglobin photodissociates with a quantum yield of $\simeq 1$.[3] Although this

(1) Haldane, J. S.; Lorrain-Smith, J. *J. Physiol. (London)* **1895**, *20*, 497.

(2) Abbreviations: HbCO and HbO_2, carboxy- and oxyhemoglobin; M(Por), metalloporphyrin; py, pyridine; TPP, tetraphenylporphyrin; DPD, deuterioporphyrin dimethyl ester.

0002-7863/81/1503-4104$01.25/0

phenomenon is commonly used as a tool with which to examine the reactions of hemoproteins and model compounds,[4] more recently, there has been increased interest in understanding the photophysical processes which underlie CO dissociation from carboxyferroporphyrins Fe(Por)(CO)[5-7] and ligand release from metalloporphyrins, in general.[8,9] However, such studies are hampered by a number of features. The intense porphyrin-like (π–π^*) absorptions make it difficult to accurately characterize the ligand field states of the metal center.[10] Ligand dissociation subsequent to photon absorption by Fe(Por)(CO) is rapid, even on the picosecond time scale,[5] precluding ready spectroscopic identification of intermediate states. The speed of the reaction makes it impossible to test proposals involving triplet excited states by quenching experiments, because even oxygen quenching would be too slow.

In the present investigation, triplet sensitization[11] is used to examine the nature and energy of the electronic state(s) involved in ligand photorelease by Fe(Por)(CO) and also to study triplet state production, using zinc porphyrin (Zn(Por)) as a closed-shell reference compound. Both processes are reversible over ordinary time scales, and thus, the classical sensitization procedures, involving product accumulation over long times, are unusable. We have therefore employed a flash photolytic sensitization procedure analogous to that used by Land and co-workers to determine triplet–triplet extinction coefficients.[12] Conditions are so arranged that the concentration of the "photoproduct", whether it be photodissociated ferroporphyrin or triplet state Zn(Por), is measured in a time short compared to its lifetime, and the relative amounts generated by direct and sensitized excitation are assessed. Through the use of an appropriate suite of donors, we show that triplet excitation can be transferred to the lowest lying Zn(Por) triplet state and to ferroporphyrin states of higher than singlet multiplicity and with energy no higher than $\sim 14\,300$ cm^{-1}. The essentially classical photochemical measurements reported here, having provided information inaccessible even to the latest picosecond technologies, are used to discuss mechanisms both for sensitized and for direct CO photorelease by ferroporphyrins.

Experimental Section

Materials. Carbon monoxide (Matheson) was pretreated with Drierite, Ascarite, and Ridox to remove H_2O, CO_2, and O_2. Toluene was purified by distillation from sodium under an atmosphere of N_2 and used immediately. Pyridine was distilled from KOH. It was chosen as nitrogenous base for coordination to the metalloporphyrins because it does not react with the sensitizers used in this study, it is a liquid which is easy to handle, it has no hydrogens susceptible to hydrogen-abstraction by photoexcited ketones, and it improved the solubility of some of the sensitizers used. Free-base tetraphenylporphyrin (TPP) and deuteroporphyrin dimethyl ester (DPD) were purchased (Alfa). Literature

Scheme I

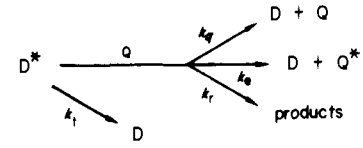

methods[13] were used for metal insertion and for the synthesis of ferroporphyrin solids Fe(DPD)(py)$_2$ and Fe(TPP)(py)$_2$. Biacetyl (Aldrich) was distilled, washed twice with small amounts of saturated sodium bicarbonate/water solution, and then dried. Eosin Y disodium salt (high purity, Aldrich) was used as received. Other sensitizers were recrystallized several times from toluene (whenever possible), cyclohexane, or benzene.

Deoxygenated solutions were prepared by five freeze–pump–thaw cycles followed by addition of an atmosphere of dry N_2, and all reactions were carried out under an atmosphere of dry N_2 unless otherwise noted. Toluene was used as solvent for these experiments, with one exception. In samples containing Eosin Y, a solution of acetonitrile, toluene, and pyridine, in a 30:20:5 ratio (v:v:v), was used as the solvent in order to obtain adequate solubility and to avoid the occurrence of Eosin Y dimers.[14] Neither optical absorption nor steady-state emission measurements as a function of [Eosin Y] indicated dimer formation in this solvent for the concentration range (10^{-7}–3×10^{-5} M) used in sensitization studies.

Solutions of Fe(Por)(py)(CO) (POR = TPP or DPD) for quantum yield measurements were prepared by adding, under N_2 purge, aliquots of a degassed solution of Fe(Por)(py)$_2$ in pyridine to a pyridine/toluene solution which had previously been degassed and then saturated with CO. Finally, an equilibrium pressure of 1 atm of CO was established by bubbling CO through the sample for 15 min ([CO] = 7.5 mM/atm at 20 °C). Final concentrations of Fe(TPP) were typically 2×10^{-6} M. Samples in which the Fe^{III}(TPP) absorption peak at 505 nm was detectable ($A \gtrsim 0.02$ optical density) were discarded. Zn(DPD)(py) and Zn(TPP)(py) samples were prepared by using the same procedure. Final concentrations of Zn(Por)(py) also were typically 2×10^{-6} M.

Quantum Yield Measurements. Quantum yields, ϕ, for CO photorelease and for Zn(Por) triplet formation were determined by using an apparatus described earlier to monitor the transient absorbance changes following flash photolysis.[15] Normally, a Xenon Corp. flash lamp assembly Model No. 457 was used as excitation source, but occasionally a Sun Pak No. 611 photographic flash was used. Light intensities were normally varied with Melles-Griot neutral density filters and monitored as described;[15] the output of the photographic flash could also be changed by varying the flash duration. For normal CO photorelease[16]

$$-\ln (1 - (\Delta A_0/\Delta A_\infty)) = \Gamma J \qquad (1)$$

where ΔA_∞ is the zero-time absorbance change upon full photolysis, ΔA_0 is the observed change for a flash of integrated intensity J, and Γ is a constant proportional to the photorelease quantum yield at the wavelength of flash excitation. ΔA_∞ is obtained either from direct difference-spectrum measurement or from a least-squares fit to eq 1 with the constraint that the theoretical line extrapolates back to an intercept of zero at $J = 0$.[15,16] Since ϕ is wavelength independent for direct CO photorelease in these systems,[3,17] eq 1 also holds in the absence of sensitizer for the broad-band flash excitation except that $\Gamma = \gamma\phi$, where γ involves a convolution of the flash lamp profile, screening, filter, and the absorbance spectrum of the particular sample. For the present purposes, it is adequate to ignore differences in γ among the different Fe(Por)(B)(CO) and MbCO since these are small. A plot according to eq 1 gives a straight line whose slope, normalized to that of MbCO ($\phi = 1$), is the

(3) (a) Warburg, O.; Negelein, E. *Biochem. Z.* **1929**, *214*, 26–63, 64–82. (b) Warburg, O.; Schocken, V. *Arch Biochem.* **1949**, *21*, 363–9. (c) Bucher, T.; Negelein, E. *Biochem. Z.* **1941**, *311*, 163–181. (d) Bucher, T.; Kaspers, J. *Biochim. Biophys. Acta* **1947**, *1*, 21–34.

(4) (a) Antonini, E.; Brunori, M. "Hemoglobin and Myoglobin in their Reactions with Ligands"; North-Holland Publishing Co.: Amsterdam, Netherlands, 1971. (b) Gibson, Q. H. "The Porphyrins"; Dolphin, D., Ed.; Academic Press, New York, 1978; Vol. V, Chapter 5. (c) Traylor, T. G.; Chang, C. K.; Geibel, J.; Berzinis, A.; Mincey, T.; Cannon, J. *J. Am. Chem. Soc.* **1979**, *101*, 6716–6731.

(5) Shank, C. V.; Ippen, E. P.; Bersohn, R. *Science (Washington, D.C.)* **1976**, *193*, 50–51.

(6) Greene, B. I.; Hochstrasser, R. M.; Weisman, R. B.; Eaton, W. A. *Proc. Natl. Acad. Sci. U.S.A.* **1978**, *75* (11), 5255–5259.

(7) Noe, L. J.; Eisert, W. G.; Rentzepis, P. M. *Proc. Natl. Acad. Sci. U.S.A.* **1978**, *75*, 573–577.

(8) Gibson, Q. H.; Hoffman, B. M. *J. Biol. Chem.* **1979**, *254*, 4691–4697.

(9) Hoffman, B. M.; Gibson, Q. H. *Proc. Natl. Acad. Sci. U.S.A.* **1978**, *75*, 21–25.

(10) Eaton, W. A.; Hanson, L. K.; Stephens, P. J.; Sutherland, J. C.; Dunn, J. B. R. *J. Am. Chem. Soc.* **1978**, *100*, 4991–5003.

(11) (a) Turro, N. J. "Modern Molecular Photochemistry"; Benjamin: Menlo Park, CA, 1978; pp 121, 181, 186, 290, 292, 350, 352. (b) Balzani, V.; Moggi, L.; Manfrin, M. F.; Bolletta, F. *Coord. Chem. Rev.* **1975**, *15*, 321–433.

(12) Amouyal, E.; Bensasson, R.; Land, E. J. *Photochem. Photobiol.* **1974**, *20*, 415–422.

(13) (a) Adler, A. D.; Longo, F. R.; Kampas, F.; Kim, J. *J. Inorg. Nucl. Chem.* **1970**, *32*, 2443–2445. (b) Epstein, L. M.; Straub, D. K.; Maricondi, C. *Inorg. Chem.* **1967**, *6*, 1720–1724. (c) Kobayashi, H.; Yanagawa, Y. *Bull. Chem. Soc. Jpn.* **1972**, *45*, 450–456.

(14) (a) Fleming, G. R.; Knight, A. W. E.; Morris, J. M.; Morrison, R. J. S.; Robinson, G. W. *J. Am. Chem. Soc.* **1977**, *99*(13), 4306–4311. (b) Marshall, K. C.; Wilkinson, F. *Leischrift Phys. Chem.* **1976**, *101*, 67–78. (c) Chrysoschoos, J. *Mol. Photochem.* **1974**, *6*, 23–42. (d) Parker, C. A.; Hatchard, C. G. *Trans. Faraday Soc.* **1961**, *57*, 1894–1904. (e) Parker, C. A.; Hatchard, C. G. *J. Phys. Chem.* **1962**, *66*, 2506–2511. (f) Kasche, V.; Lindquist, L. *Photochem. Photobiol.* **1965**, *4*, 923–933.

(15) Stanford, M. A.; Swartz, J. C.; Phillips, T. E.; Hoffman, B. M. *J. Am. Chem. Soc.* **1980**, *102*, 4492–4498.

(16) Brunori, M.; Giacometti, G. M.; Antonini, E.; Wyman, J. *Proc. Natl. Acad. Sci. U.S.A.* **1973**, *70*, 3141–3144.

(17) See: Saffran, W. A.; Gibson, Q. H. *J. Biol. Chem.* **1977**, *252*, 7955–7958.

Table I. Triplet State Quenching by Metalloporphyrin

Anthracene[a]

	$\bar{k}_1$, s^{-1}	$10^{-9}k_Q$, M^{-1} s^{-1}
Fe(TPP)(py)(CO)	1080	6.9
$Fe(TPP)(py)_2$	1020	6.3

Biacetyl[b]

	Stern–Volmer slope	$10^{-9}k_Q$, M^{-1} s^{-1}
Fe(TPP)(py)(CO)	2.0×10^6	4.0
Zn(TPP)(py)	3.0×10^6	6.0

[a] Obtained from fitting triplet-triplet absorption decay rate constants to eq 3. [b] Obtained by fitting steady-state phosphorescence to eq 4 and assuming $\tau = 0.5$ ms.[21]

apparent quantum yield. The effect of an added triplet sensitizer was obtained by measuring the quantum yield for a sample without donor, ϕ_0, and then remeasuring the donor-dependent apparent quantum yield, ϕ(D), after addition by airtight syringe of known small volumes (typically <50 μL) of sensitizer in a deoxygenated toluene solution. We verified that ϕ(D) is a well-defined quantity by confirming that plots according to eq 1 remain linear upon addition of donor and that they depend only upon the integrated flash intensity (J) and not separately on the photon flux or flash duration. Although absolute quantum yields were estimated relative to that of MbCO, typically, we are interested in the ratio of the quantum yield at some donor concentration to that in the absence of the donor.

$$F(\mathrm{D}) = \phi(\mathrm{D})/\phi_0 \qquad (2)$$

For sensitizers whose absorption maxima lie to the blue of the M(Por) Soret band, a Corning blue filter No. 7-54, transmitting mainly between 290 and 380 nm, was used to minimize the photolysis pulse directly absorbed by the metalloporphyrin. For Eosin Y as donor, the combination of Corning No. 4-96 and a Melles-Griot No. 03FCG067 filters, transmitting roughly between 475 and 600 nm, was employed for this purpose. Transient changes in absorption following photolysis of Fe(TPP)(py)(CO) solutions were monitored[15] at ~440 nm, to the red of the absorption bands at most of the sensitizers used and to the blue of the Eosin Y absorption. Fe(DPD)(py)(CO) samples were monitored at ~435 nm. Kinetics of Zn(Por) triplet decay[18,19] were monitored at ~450 nm, far to the red of the absorption of all sensitizers used, again with the exception of Eosin Y.

Steady-State Triplet Quenching. Steady-state emission measurements were made by using an Hitachi MPF-2A fluorescence spectrophotometer. An Hamamatsu No. R818 red-extended phototube was employed to monitor emission at long wavelengths.

Results

Triplet State Quenching by Metalloporphyrins. A sensitizer triplet state (D*) in solution with a metalloporphyrin quencher (Q) can have several fates (Scheme I).[11] Control experiments gave no evidence for the occurrence of side reactions, labeled with rate constant k_r in Scheme I. All the sensitizers employed were photostable in CO-saturated pyridine/toluene solutions, and there were no ground-state or light-induced chemical reactions between sensitizer and metalloporphyrin. In particular, metalloporphyrin ground-state spectra, kinetic difference spectra, and CO-rebinding rates[15] all remained unchanged by addition of sensitizers.

The remaining processes combine to give the observed overall rate constant for quenching of the donor triplet by a metalloporphyrin k_Q. Quenching of the anthracene triplet state by ferroporphyrins was measured kinetically. First-order triplet state decay rates were obtained by monitoring the anthracene triplet–triplet absorption progress curves at 424 nm[20] subsequent to a flash ([anthracene] = 10^{-4} M). During these experiments we measured the fractional triplet population created by excitation of anthracene (10^{-4} M) through the Corning 7-54 filter to be a few tenths of a percent, depending on the extinction coefficient employed.[20]

In the presence of M(Por) quencher, such rates are expected to follow relationship 3,[11] and the addition of Fe(TPP)(py)(CO)

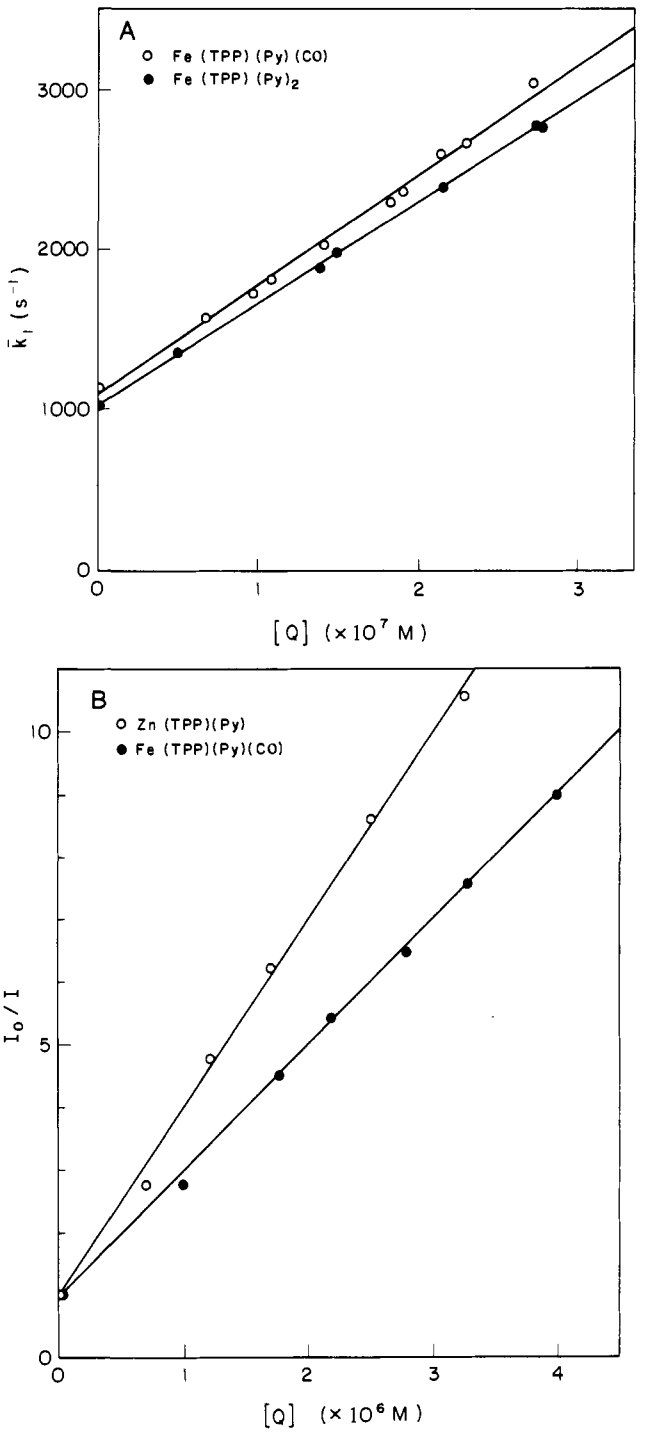

Figure 1. A. Anthracene triplet decay rate as a function of quencher concentration (eq 3). Excitation source: xenon flash lamp screened from sample by Corning blue-filter No. 7-54. Absorbance was monitored at 424 nm. Quencher = Fe(TPP)(py)(CO) (○); quencher = $Fe(TPP)(py)_2$ (●). Conditions: [anthracene] = 1×10^{-4} M; [py] = 1.0 M; toluene; 21 °C; Fe(TPP)(py)(CO) samples under 1 atm of CO; $Fe(TPP)(py)_2$ samples under 1 atm of N_2. B. Stern–Volmer plots according to eq 4 for quenching of biacetyl phosphorescence intensity, I, observed under steady-state illumination. Quencher: Fe(TPP)(py)(CO) (●); Zn(TPP)(py) (○). Conditions: [py] = 1.0 M; [CO] = 7.5×10^{-3} M; toluene; 21 °C for all samples; [biacetyl] = 0.001 M. Straight lines were generated by linear least squares fit to eq 4.

(18) (a) Pekkarinen, L.; Linschitz, H. *J. Am. Chem. Soc.* **1960**, *82*, 2407–2411. (b) Carapellucci, P. A.; Mauzerall, D. *Ann. N.Y. Acad. Sci.* **1975**, *244*, 214–238.

(19) Zemel, H.; Hoffman, B. M. *J. Am. Chem. Soc.* **1981**, *103*, 1192–1201.

(20) (a) Lindquist, L.; Tfibel, F. *Chem. Phys.* **1975**, *10*, 471–478. (b) Meyer, Y. H.; Astier, R.; Leclerq, J. M. *J. Chem. Phys.* **1972**, *56*, 801–815.

$$\bar{k}_1 = k_1 + k_Q[Q] \quad (3)$$

and $Fe(TPP)(py)_2$ to anthracene samples caused the observed anthracene triplet decay rate to increase linearly with the porphyrin concentration as predicted (Figure 1A). Least-squares fitting the data to eq 3 gives the quenching rates listed in Table I. They are effectively the same for the two porphyrins, approaching the diffusion-controlled limit, $\sim 10^{10}$ M^{-1} s^{-1} in toluene at room temperature. Thus, a carbonylferroporphyrin is not uniquely effective as a triplet quencher.

The unimolecular decay rate for the anthracene triplet, k_1, is also the same for both sets of measurements: $k_1 \approx 10^3$ s^{-1}, noticeably higher than the intrinsic value.[18,19] This discrepancy is a common occurrence and is probably due to the presence of residual O_2. Diffusion-controlled quenching by $\sim 10^{-7}$ M O_2 would give the observed rate. Because experiments with Fe(Por)(py)(CO) had to be run under an appreciable CO pressure and thus samples could not be sealed off after freeze–pump–thaw degassing, this residual oxygen could not be eliminated. However, many observations showed the residual O_2 level to be essentially constant, and thus its only effect is to reduce the effective triplet lifetime by a fixed, known amount.

Biacetyl is one of the few organic molecules whose phosphorescence is observable in normal fluid solution at room temperature,[21] and we used steady-state phosphorescence measurements to obtain the rate constant for the quenching of the biacetyl triplet by Fe(TPP)(py)(CO) and by Zn(TPP)(py). Plots of I_0/I, where I and I_0 are the phosphorescence intensity in the presence and absence of quencher, vs. [M(Por)] obey the linear, Stern-Volmer relation[11] (4) as seen in Figure 1B. From the slopes of

$$I_0/I = 1 + k_Q\tau[M(Por)] \quad (4)$$

the plots calculated by least-squares fitting to eq 4 and the reported lifetime of the biacetyl triplet,[21a] $\tau = 0.5$ ms, the values of k_Q presented in Table I were obtained. The slopes in Figure 1B and the calculated quenching rate constants for the carbonylferroporphyrin and for the closed-shell zinc porphyrin are again so similar that they indicate that the quenching process is independent of the metal. The rate constants calculated for biacetyl triplet quenching appears to be slightly lower than those measured for quenching of the anthracene triplet. This most likely reflects uncertainties in the value of τ used to obtain k_Q from eq 4, rather than any significant differences in k_Q.

Energy Transfer: Observation. Figure 2 presents the Soret region absorption spectra of Fe(TPP)(py)(CO) and Zn(TPP)(py) and the profile of the Xe flash lamp screened by the 7-54 color filter. It is clear that flash photolysis through the filter will excite a UV absorbing donor with appreciable selectivity, relative to the Fe(Por). Unless explicitly noted all results presented here involve the use of the 7-54 filter.

Figure 3A presents transient absorbance progress curves following photolysis of Fe(TPP)(py)(CO). In experiments, such as these, in which high pyridine concentration is employed, it is well established that the observed photoproduct is $Fe(TPP)(py)_2$ and the photolysis and CO recombination reactions observed have the stoichiometry[4c,15,22]

$$\text{photolysis: } Fe(Por)(py)(CO) \xrightarrow{h\nu} Fe(Por)(py) + CO \xrightarrow[\text{rapid}]{py} Fe(Por)(py)_2 + CO$$

$$\text{recombination: } Fe(Por)(py)_2 \xrightarrow{CO} Fe(Por)(py)(CO) + py$$

Least-squares fitting of the decay trace gives the zero-time absorbance change, ΔA_0, and the pseudo-first-order recombination rate, which is inversely related to [pyridine] and proportional to [CO].[15,22] The absorbance change upon complete photolysis, ΔA_∞, was measured either from the static difference spectrum obtained upon addition of CO to the $Fe(Por)(B)_2$ sample or from eq 1 in the course of a quantum yield analysis (see above).

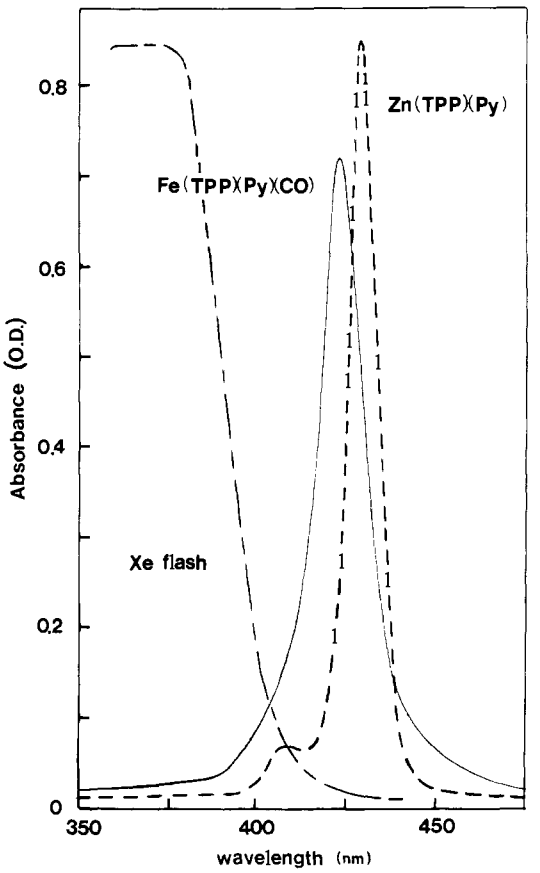

Figure 2. Absorption spectra: [Fe(TPP)(py)(CO)] = 2.9×10^{-6} M (—); [Zn(TPP)(py)] = 1.9×10^{-6} M (---). Conditions: [py] = 1 M, [CO] = 7.5×10^{-3} M, toluene; 21 °C. Profile of Xe flash was screened by 7-54 color filter, as monitored by a 1P28 photomultiplier (uncorrected) (— - —).

The trace in Figure 3B was obtained upon photolysis following addition of 10^{-4} M anthracene, all other conditions being identical. Going from part A to part B in Figure 3, the value of ΔA_0 is roughly doubled. However, in this and all other experiments, addition of sensitizer caused no change in the ferroporphyrin transient difference spectrum, and the pseudo-first-order CO–recombination rate was also unchanged. We conclude that the increased magnitude of the transient absorbance in Figure 3B results from photosensitization of CO photorelease by anthracene. More effective sensitization could be achieved by using the photoflash; comparison of parts D and E in Figure 3 shows that photodissociation is increased by approximately ninefold upon addition of sensitizer. This set of traces shows a larger effect because the photoflash emission has a more favorable overlap with the sensitizer absorption band. Despite this, the photoflash was not used in other experiments because its long duration (600 μs), compared to that of the Xenon Corp. flash (20 μs) precluded satisfactory monitoring of Zn(Por) triplet formation in an analogous fashion.

Addition of small amounts of O_2 ($\sim 10^{-5}$ M in solution) abolishes the sensitized component of traces B and E in Figure 3 and returns the observed transient absorbance curves to parts A and D, respectively, in Figure 3. This addition does not change the kinetic difference spectrum or the CO-rebinding rate, indicating that O_2 does not act as a ligand and there is no loss of ferroporphyrin through irreversible oxidation. Upon thoroughly purging the sample with CO, sensitization is reinstated as seen in parts C and F of Figure 3. We conclude that the effect of oxygen is to quench the donor triplets, thus proving that the sensitization occurs solely via triplet energy transfer. Since these

(21) (a) Calvert, J. G.; Pitts, J. N. "Photochemistry"; Wiley: New York, 1966, pp 323–336. (b) Scandola, M. A.; Scandola, F. *J. Am. Chem. Soc.* **1970**, *92*, 7278–7281. (c) Sandros, K. *Acta Chem. Scand.* **1973**, *27*, 3021–3032.

(22) White, D. K.; Cannon, J. B.; Traylor, T. G. *J. Am. Chem. Soc.* **1979**, *101*, 2443–2454.

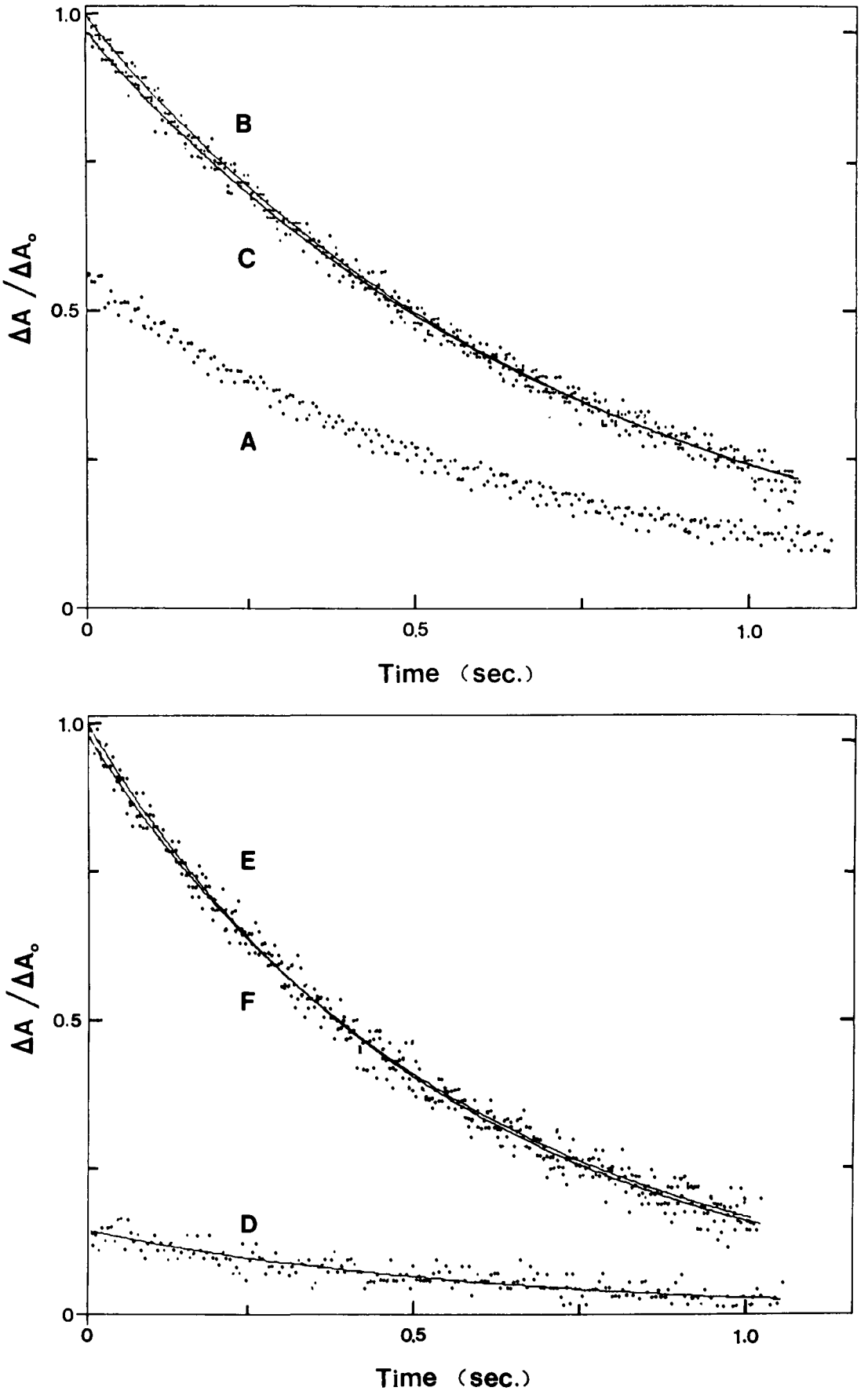

Figure 3. Kinetic traces of relative absorbance change ($\Delta A/\Delta A_0$) for CO recombination after flash photolysis of Fe(TPP)(py)(CO): upper panel, flash excitation by Xenon Corp. flash assembly; lower panel, by photographic flash, both screened by Corning No. 7-54 filter. Sequence of traces is as follows: freshly prepared sample, without sensitizer (*A*, D); sensitizer added, 2.2×10^{-4} M Michler's Ketone (B); 1×10^{-4} M anthracene (*E*); added oxygen (0.03 atm) returns traces to (A, D); thorough deoxygenation produces C and F. Conditions: [CO] = 7.5×10^{-3} M, [Fe(TPP)] = 2×10^{-6} M, 440 nm, 2-nm slit width, toluene, 21 °C. Upper panel: [py] = 1 M; Lower panel: [py] = 0.7 M.

Table II. Quasi Time-Resolved Sensitization Data

triplet energy donor	donor properties: triplet symmetry	ϕ_{isc}	$E_{triplet}$ kcal/mol, 10^3 cm^{-3}	sensitization results[a]: $[D_m]$, M	Zn(Por) F_m	Zn(Por) A	Fe(Por)(CO) F_m	Fe(Por)(CO) A
Michler's ketone[b]	$^3(n, \pi^*)$	1.0	61.0, 21.4	2.2×10^{-4}	4.1	8.4	1.6	1.6
fluorenone[c]	$^3(n, \pi^*)$	0.93	53.3, 18.7	1×10^{-3}	2.6	4.3	1.4	1.1
acridine[d]	$^3(\pi, \pi^*)$	0.7	45.0, 15.8	3×10^{-5}	3.9	7.9	1.6	1.6
anthracene[e]	$^3(\pi, \pi^*)$	0.70	42, 14.9	1×10^{-4}	2.7	4.6	1.9	2.4
eosin Y[f]	$^3(\pi, \pi^*)$	0.7	40.9, 14.3	1×10^{-5}	2.7	4.6	1.6	1.6

[a] F_m is the maximum donor-dependent quantum yield ratio observed at donor concentration $[D_m]$, as discussed in the text. A is defined by eq 5 and obtained from eq A13, as described. For Michler's ketone and fluorenone as sensitizer, both Fe(TPP) and Fe(DPD) were used with identical results. In all other cases, Por = TPP. [b] See ref 23. [c] See ref 24. [d] See ref 14a, 24a,b, and 25. [e] See ref 20. [f] See ref 14.

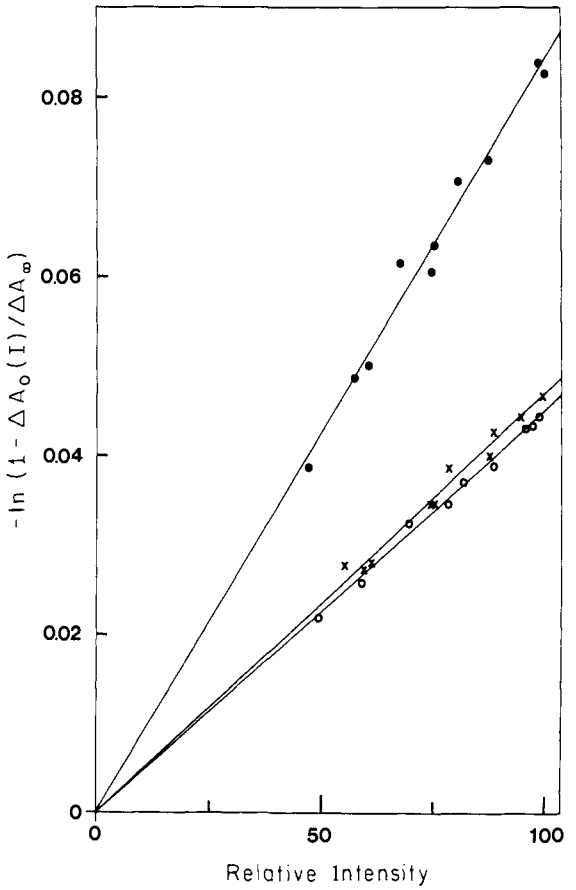

Figure 4. CO release quantum yield plots according to eq 1 for Fe(TPP)(py)(CO) sample before (○) and after (●) the addition of 1×10^{-4} M anthracene. Straight lines are generated from data through linear least-squares fit. Flash excitation source: xenon flash lamp screened from sample by Corning No. 7-54 blue filter. Conditions: [Fe(TPP)] = 2×10^{-6} M; [py] = 1.0 M; [CO] = 7.5×10^{-3} M; toluene, 21 °C. The quantum yield plot for Mb ($\phi = 1$) is shown for reference (X). Conditions: [Mb] = 5×10^{-6} M; 0.05 M tris buffer, pH 7.0, [CO] = 1.0×10^{-3} M.

measurements involved a time-resolved observation of the non-steady-state-sensitized CO photorelease and rebinding, yet the actual buildup of photoproduct is not monitored, only the total amount, it is appropriate to call the process quasi-time-resolved (QTR) triplet sensitization.

Quantitative treatment of the phenomenon of triplet sensitized CO photodissociation is best couched in terms of the donor concentration-dependent apparent quantum yield for CO photorelease, $\phi(D)$. Representative quantum yield measurements for Mb(CO), for Fe(TPP)(py)(CO), and for the latter in the presence of 10^{-4} M anthracene are shown in Figure 4. The dependence of $-\ln (1 - (\Delta A_0/\Delta A_\infty))$ on the integrated flash intensity, J, is clearly linear in the presence as well as in the absence of donor, and the roughly twofold increase in slope caused by the donor parallels

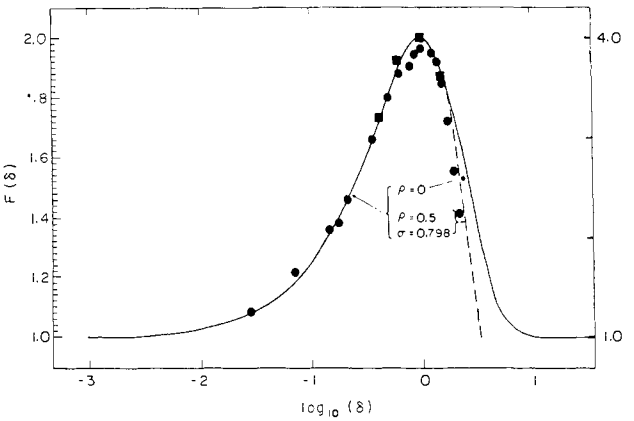

Figure 5. Quantum yield ratios, $F(D)$ (eq 2), as a function of concentration of anthracene as donor. Donor concentration is expressed as $\delta = D/D_m$ (see text), where $D_m = 1 \times 10^{-4}$ M. Curves drawn through data points are drawn according to eq A13 with $A = 2.72$ (—) and according to eq A15 with $\rho = 0.5$ and $\sigma = 0.798$ (---). Quantum yields for CO release from Fe(TPP)(py)(CO) were monitored at 440 nm (●), left-hand ordinate; quantum yields for Zn(TPP)(py) triplet production were monitored at 450 nm (■), right-hand ordinate. Excitation source: xenon flash lamp screened from sample by Corning blue filter No. 7-54. Conditions: [py] = 1.0 M; [CO] = 7.5×10^{-3} M; toluene; 21 °C; [Por] = 2×10^{-6} M.

the ca. twofold increase in ΔA_0 observed directly in Figure 3.

Figure 5 presents a plot of the triplet sensitized enhancement of the quantum yield, $F(D)$ (eq 2), obtained from a series of quantum yield measurements with differing donor concentrations. As the concentration is raised, $F(D)$ gradually rises until it reaches a maximum value, ~2 in this case, at $[D] \equiv [D_m]$. A further increase in [D] causes a precipitous reduction in F.

In order to characterize the mechanism of triplet sensitization, we substituted Zn(Por)(py) for the carbonylferroporphyrin in control samples which were identical in all other respects. Zn(Por) is known to accept triplet energy from a variety of sensitizer molecules, and Zn(Por) triplets have long lifetimes with known decay constants[18,19] (k(first-order decay) $\simeq 100$ s^{-1}; k(second-order decay) $\simeq 10^9$ M^{-1} s^{-1}; $k(O_2$ quench) $\simeq 10^{10}$ M^{-1} s^{-1}). The concentration of Zn(Por) triplets and the triplet decay rate were obtained by monitoring the triplet–triplet absorbance after photolysis. In our experiments, the Zn(Por) triplets exhibit a first-order decay whose rate constant ($k \approx 10^3$ s^{-1}); this is probably determined by quenching from the residual O_2, just as observed above for the anthracene triplets.

The photosensitized formation of the Zn(Por) triplet state behaves similarly to that of CO photorelease. This is shown in Figure 5, in which the relative quantum yield for Zn(Por) production is also plotted. Triplet production reaches its maximum value at the same donor concentration as does that for CO photodissociation, but the measured maximum enhancement of "photoproduct" formation is roughly twofold greater for Zn(Por) triplet formation than it is for photorelease (Table II). At least a part of this difference is simply explained by noting that all experiments were run at the same metalloporphyrin concentration

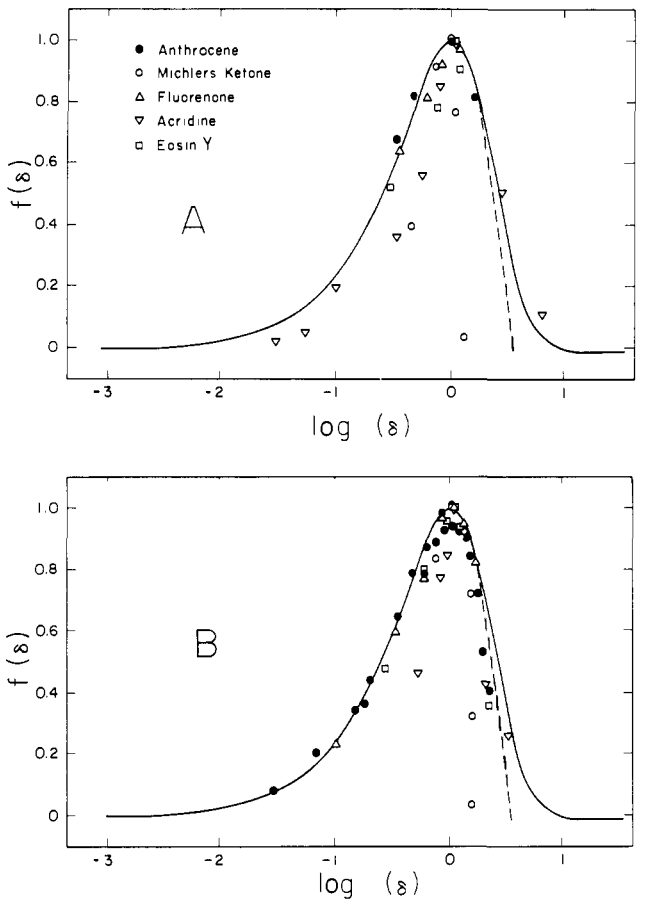

Figure 6. Quantum yield ratios $f(\delta)$ (eq 5) as a function of log of normalized donor concentration for five energy donors. (A) Quantum yield ratios for Zn(TPP)(py) triplet production monitored at 450 nm. Theoretical curve calculated from eq A13 and 5 for $\rho = 0$ (—) and from eq A15 and 5 for $\rho = 0.5$ and $\sigma = 0.798$ (---). (B) Quantum yield ratios for CO release from Fe(TPP)(py)(CO) monitored at 440 nm. Theoretical curves are calculated from eq A13 and 5 (—) and from eq A15 and 5 for $\rho = 0.5$ and $\sigma = 0.914$ (---).

($\sim 2.6 \times 10^{-6}$ M) but that in the vicinity of the maximum of the excitation profile, ~350 nm, the extinction coefficient of Zn(Por)(py) is lower than that of Fe(Por)(py)(CO) (Figure 2). It is intuitively clear (and is shown rigorously below) that the ratio of photoproduct formed in the presence of a sensitizer to that formed in its absence must vary inversely with the absorbance of the M(Por) in question. Thus, sensitization of CO photorelease and of Zn(Por) triplet formation by triplet anthracene occur with comparable efficiency.

Table II summarizes the sensitization results for anthracene and other energy donors, along with the pertinent data regarding their excited states; included are the maximum value of the relative quantum yield, F_m, and the concentration, $[D_m]$, of this maximum. The F_m varies somewhat but probably not significantly, with donor D, and the ca. twofold difference between F_m for the two photoprocesses, discussed above for anthracene, is also a common feature. In all cases the same general dependence of $F(D)$ on [D] is observed. This is clearly shown in Figure 6, in which the abscissa is log δ, $\delta = [D]/[D_m]$ and the ordinate is a normalized relative quantum yield

$$f(\delta) = \frac{F(\delta) - 1}{F_m - 1} \qquad (5)$$

The data may be summarized as follows. The efficiency of triplet sensitized CO photorelease by a carbonylferroporphyrin, as measured by F_m, is not dependent on the nature of the donor triplet state ($(n-\pi)^*$ or $(\pi-\pi)^*$), is comparable to that of Zn(Por) triplet formation and is roughly the same for donors whose triplet states are appreciably higher in energy than the lowest porphyrin-like singlet states and for at least two which are significantly lower in energy (Figure 7).[10,14,18,23-25] Since energy transfer falls off sharply if the donor energy is lowered until it approaches that of the acceptor,[24c] these results indicate that sensitized CO photorelease can occur through triplet energy transfer to a state(s) of the carbonylferroporphyrin with energy less than 14 300 cm^{-1}, the triplet energy of Eosin Y.[14] The observation that the degree of Zn(Por) triplet formation and of CO photorelease (when corrected for absorbance) are comparable indicates that bond dissociation following triplet energy transfer must occur with high efficiency. In the following section we put these conclusions on a more rigorous footing.

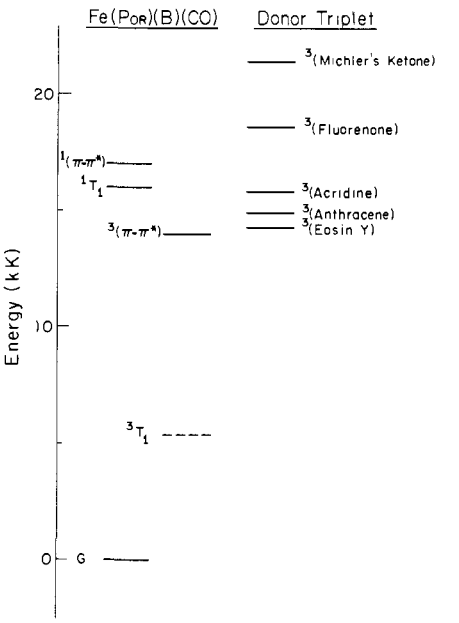

Figure 7. Diagram of energy levels for carbonylferroporphyrin acceptor (left) and triplet energy levels of donor molecules used (right). Donor energies are given in Table I. The $^1(\pi,\pi^*)$ and $^1T_1$ levels are those for HbCO as reported in ref 10. The $^3(\pi-\pi^*)$ level is placed at the energy found in Zn(TPP)(py), and the energy of $^3T_1$ is calculated from $^1T_1$ by using the exchange correction of ref 10.

Scheme II

$$D \xrightarrow{h\nu} D^*$$
$$Q + D^* \xrightarrow{k_e} Q^* + D$$
$$Q \xrightarrow{h\nu} Q^*$$
$$D^* \xrightarrow{k_1} D$$
$$Q^* \xrightarrow{k_g} Q$$

Analysis of QTR Energy Transfer. In this section we present equations for the apparent photoreaction quantum yield for the "excitation" of compound Q by flash photolysis in the presence of triplet sensitizer D. The reactions that need to be considered are shown in Scheme II. Here we may equally well have Q = Fe(Por)(py)(CO) and Q* = Fe(Por)(py)$_2$ or Q = Zn(Por)(py) and Q* = 3(Zn(Por)(py))*. The experimental arrangement is of course designed to minimize direct excitations of Q and to maximize the formation of D* and thus photoproduct formation

(23) (a) Wolf, M. W.; Legg, K. D.; Brown, R. E.; Singer, L. A.; Parks, J. H. *J. Am. Chem. Soc.* **1975**, *97*, 4490–4497. (b) Schuster, D. I.; Goldstein, M. D.; Bane, P. *Ibid.* **1977**, *99*, 187–193.

(24) (a) Birks, J. B. "Organic Molecular Photochemistry"; Wiley: London, 1973; Vol. I, pp 10, 19–21, 26, 308–345. (b) Birks, J. B. "Organic Molecular Photochemistry"; Wiley: London, 1975; Vol. II, pp 128–133, 144–147, 150, 153, 481. (c) Lamola, A. A.; Turro, N. J. "Energy Transfer and Organic Photochemistry"; Wiley: New York, 1969, Vol. XIV, pp 92–93, 106, 117, 175, 200–201, 220.

(25) (a) Kellmann, A. *J. Phys. Chem.* **1977**, *81*, 1195–1198. (b) Wilkinson, F.; Farmilo, A. *J. Chem. Soc., Faraday Trans. 2* **1978**, *74*, 2083–2091.

by energy transfer (rate constant k_e). The D* decay rate, $\bar{k}_1$, includes all processes by which Q quenches D*, including those which do not lead to formation of Q*. (See Appendix.)

If we consider an excitation source with arbitrary shape $I(t)$ and total duration, τ, then the time course of a flash photolytic reaction may be divided into domains.

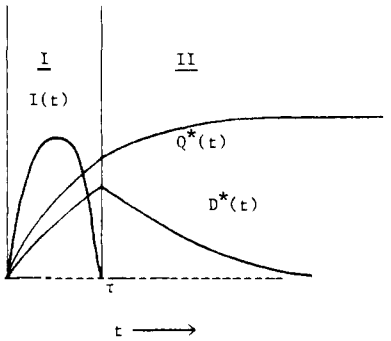

For $t < \tau$, D* and Q* are generated by direct excitation and Q* is also produced by energy transfer from D*. For $t > \tau$, D* decays with a rate constant $\bar{k}_1$, while continuing to generate Q* by energy transfer. At any given time, the concentration of Q* is determined by a balance between excitation processes and the decay process of rate k_g.

In a general time-resolved (TR) sensitization experiment, Q* might be measured at any time t. In particular, for $\tau < t \leq 1/k_1$ one would observe interplay between the creation of Q* by energy transfer and the return to the initial state Q. Such experiments will be reported in a later publication. In the present experiments, observation is restricted to time $t >> 1/\bar{k}_1$, when all D* has disappeared and sensitized creation of Q* has ceased. However, the Q* and D* decay rates also satisfy the inequality, $\bar{k}_g << k_1$, (here $k_g \simeq 10^{-4}\ k_1$), and therefore there is no appreciable loss of Q* during the sensitization process. These two inequalities define the quasi-time-resolved (QTR) sensitization process.

In a QTR experiment, the values of ΔA_0 obtained by fitting the photoproduct decay trace to a single exponential is simply a sum of the contributions from sensitized and direct photolysis. As shown in the Appendix, the functional form of the eq 1, relating fraction photolysis and flash intensity, is not altered by sensitization, but becomes

$$-\ln\,(1 - (\Delta A/\Delta A_\infty)) \equiv \Omega(J,[\mathrm{D}]) = \Gamma(\mathrm{D})J \qquad (A10)$$

The proportionality constant

$$\Gamma(\mathrm{D}) = \omega_Q e^{-\epsilon_Q^D l[\mathrm{D}]} + \frac{k_e}{k_1}\omega_D[\mathrm{D}]e^{-\epsilon_D^D l[\mathrm{D}]} \qquad (A11)$$

is the apparent quantum yield, with the two terms representing direct and sensitized excitation of Q, respectively. The parameters ω_α represent the effective quantum yield for excitation or reaction of species α caused by direct light absorption. For monochromatic incident light they equal the product of the true quantum yield for direct excitation times the extinction coefficient; for broad-band illumination they involve a convolution over the flash profile, filter absorbance curves, and absorption spectra of species α. Since experimental conditions involve high donor concentrations, attenuation of the incident flux at the position of the analyzing beam through absorption by the donor is explicitly accounted for by the term $\exp(-\epsilon_\alpha^D l[\mathrm{D}])$; the actinic light strikes the cuvette face at right angles to the analyzing beam and l is the distance from the face to the analyzing beam. For monochromatic actinic light of wavelength λ, $\epsilon_D^D = \epsilon_Q^D = \epsilon^D(\lambda)$ is simply determined by the absorption of the donor at the exciting wavelength. With broad-band illumination as employed here, for the purposes of the present discussion it is adequate to consider ϵ_α^D to be an effective absorbance by the donor appropriately convoluted over the absorption band of species α. The results of our experiments are typically discussed in terms of $F(\mathrm{D})$, the ratio of quantum yields relative to that in the absence of donor (eq 2), whose theoretical expression is given by eq A12.

In the case where the absorption band of D does not overlap that of Q ($\epsilon_Q^D = 0$) the quantum yield function has a maximum at $[\mathrm{D_m}] = [\mathrm{D_m}^0] = (\epsilon_D^D l)^{-1}$ and becomes a universal function of the normalized donor concentration $\delta = [\mathrm{D}]/[\mathrm{D_m}]$

$$F^0(\delta) = 1 + A^0\delta e^{-\delta} \qquad (A13)$$

where the energy-transfer parameter, A^0, is given by eq A14 and the maximum ratio is simply

$$F_m^0 = F(\delta = 1) = 1 + A^0 e^{-1} \qquad (6)$$

As seen in Figure 5, the general shape of the $F(\mathrm{D})$ curve for anthracene is remarkably well approximated by the equations presented here. In fact, the shape of the curves for all donors, for both CO photorelease and Zn(Por) excitation, is well approximated. This is shown in Figure 6 which plots the experimental values of $f(\delta)$, as defined in eq 5, and the theoretical curve, $f(\delta) = \delta e^{-\delta}$, obtained analogously from eq A13. In all cases, the quantum yield ratio increases with sensitizer concentration, reaches a maximum at a concentration, $[\mathrm{D_m}]$, which is specific to the sensitizer but independent of the photoreaction which is being sensitized, and then decreases as the photolysis light is increasingly screened by optical absorption of the donor. For each sensitizer, this apparent decrease in quantum yield occurs after the addition of enough sensitizer to reach an optical density of approximately 2 in the wavelength range of the exciting light. Thus, $[\mathrm{D_m}]$ clearly depends upon the donor extinction coefficient in the manner predicted above.

Although the present results are largely explained by the above equations, for $\delta > 1$, the universal curve, $F^0(\delta)$, does not fall as steeply as do the experimental values. This can be understood by noting that the porphyrin absorption is in fact nonzero in the wavelength range of the excitation source ($\epsilon_Q^D > 0$). In this case (see Appendix), when $\rho = \epsilon_Q^D/\epsilon_D^D > 0$, the concentration, $[\mathrm{D_m}]$, at which $F(\mathrm{D})$ reaches its maximum is reduced from $[\mathrm{D_m}^0]$; $[\mathrm{D_m}]/[\mathrm{D_m}^0] \equiv \sigma \leq 1$. $F(\mathrm{D})$ may again be rewritten in terms of a normalized concentration, $\delta = [\mathrm{D}]/[\mathrm{D_m}]$, defined so that $F(\delta = 1) = F_m$ (eq A15). As shown in the Appendix, the sensitization parameter which we wish to obtain from experiment becomes

$$A = \frac{k_e}{\bar{k}_1}\frac{\omega_D}{\omega_Q}[\mathrm{D_m}] \qquad (7)$$

As seen in Figures 5 and 6 the inclusion of a nonzero ρ has no effect on the shape of $f(\delta)$ for $\delta < 1$ but significantly improves the correspondence with experiment for $\delta > 1$ by steepening the decrease and by predicting a fall below unity as δ gets large. However, by $\delta > 2$ the effects of a finite width of the analyzing beam introduces further complications without adding new information. Moreover, the sample calculations indicate that the value of A^0 (eq A14) obtained from eq 6 and the value of A (eq 7) obtained from the more general equation (A15) do not differ significantly (Figures 5 and 6). Thus, in subsequent analyses of the sensitization results we treat the observed F_m with eq 6 but use eq 7 to interpret the energy-transfer parameter.

By combining results presented in the quenching section with the quantum yields for sensitized photorelease, it is possible to calculate a value of the rate constant for photoproduct formation by anthracene sensitization. Rearranging eq 7 gives

$$k_e = \frac{A\bar{k}_1}{\mathrm{D_m}(\omega_D/\omega_Q)} \qquad (7a)$$

In the sensitization experiment, the porphyrin concentration was fixed at 2×10^{-6} M, at which value quenching is the dominant mode of anthracene triplet decay: $\bar{k}_1 \simeq k_Q \times 2 \times 10^{-6} \simeq 1.4 \times 10^4\ \mathrm{s^{-1}}$. Consideration of the absorbance spectra of anthracene[20a] and Fe(TPP)(py)(CO)[13] and the flash profile (Figure 2) suggest that $\omega_D/\omega_Q < 5$. Inserting these values into eq 7 along with $[\mathrm{D_m}] = 10^{-4}$ M and $A = 2.4$ (Table II), one obtains the approximate value $k_e > 6 \times 10^7\ \mathrm{M^{-1}\ s^{-1}}$.

The values of $[\mathrm{D_m}]$ for the several sensitizers vary over a span of ~30-fold and the ratio of ω_D/ω_Q must also vary substantially; thus, the apparently common sensitizing ability for a set of donors,

suggested by the roughly constant values of F_m and A, might be masking substantial variations in k_e. However, consideration of the physical meaning of $[D_m]$ and ω_D shows that their product should be roughly constant, and for the present we shall accept these results at face value. Future experiments with fully TR sensitization and monochromatic actinic light will explore this question.

One measure of the efficiency of photoproduct formation is the ratio of energy transfer and total quenching rate constants: $\eta = k_e/k_Q$. Thus, for anthracene sensitization, $\eta \gtrsim 10^{-2}$. This low estimated efficiency is *not* the result of energy wastage subsequent to energy transfer to the carbonylferroporphyrin and prior to CO photorelease. Instead, it is caused by direct quenching, presumably through exciplex formation[11,26] or other processes.[27] This conclusion is reached by calculating k_e for Zn(Por) triplet sensitization. The values for A for triplet formation are, on average, about fourfold larger than those for CO photorelease. In the calculation of k_e from eq 7, this small difference is partially balanced by a corresponding difference in ω_D/ω_{Fe} (see above). Thus, $k_e(Zn)/k_e(Fe) \approx 2$. Since the formation of triplet Zn(Por) by triplet energy transfer from a triplet anthracene energy donor must by definition have a unit efficiency per triplet quantum actually transferred, the efficiency of CO photorelease per triplet quantum transferred to a carbonylferroporphyrin is probably ca. 0.5.

Discussion

Light absorption by carbonylferroporphyrin creates a $^1(\pi-\pi^*)$ excitation, the lowest of which has energy $\sim 17\,000$ cm^{-1}; CO release probably follows within ~ 0.5 ps,[5] although slightly longer estimates have been published.[6,7] The question to be addressed is which states are involved in the process by which excitation of the porphyrin π-electron system leads to rupture of the Fe–CO bond. The discussion will be conducted in the framework provided by a partial energy level diagram (Figure 7) whose essential features are derived from the results of Eaton et al.[10]

Shank et al.,[5] following the calculations of Zerner et al.,[28] suggested that the initial porphyrin $^1(\pi \rightarrow \pi^*)$ excitation decays to a dissociating ($d_\pi \rightarrow d_{z^2}$) ligand field excitation. However, as shown by optical absorption measurements, at the ground-state geometry, this singlet state is too high in energy to be involved, and theory shows the same to be true for the triplet.[10] Thus, adopting such an interpretation would require the further assumption that dissociation involves level crossing on the way to, or at, the relaxed geometry.[29] A version of this model appears to underlie the analysis of Noe et al.,[7] who suggest that photorelease involves predissociation, with a level crossing at $\sim 16\,260$ cm^{-1} (615 nm).

Green et al.[6] interpreted their measurements differently, utilizing the energy level scheme which we also have adopted. They suggested that the porphyrin-like $^1(\pi \rightarrow \pi^*)$ levels undergo rapid internal conversion to the lowest singlet state, the $^1T_1$ crystal field state located at $\sim 16\,000$ cm^{-1}.[10] They further proposed that roughly 50% of the molecules in this state dissociate and that the rest relax to $^3T_1$, which should be only weakly dissociating at most and to the ground state.

In an earlier publication we noted that dissociation might in fact occur from the lowest $(\pi-\pi^*)$ configuration, either directly from the singlet state or from the triplet state after intersystem crossing.[9] This scheme was in part suggested by electronic structure calculations. A considerable stabilization of the Fe–CO bond apparently arises from π-back-bonding from the (d_{xz}, d_{yz}) orbitals, with donation in turn into these d_π orbitals from the highest filled porphyrin π levels.[10,28,30] Thus, an excitation which is nominally associated with the porphyrin π system could nonetheless decrease the Fe–CO bond strength significantly.

The results presented here show that energy transfer to a state(s) of energy lower than $\sim 14\,300$ cm^{-1} (E_1 of Eosin Y) causes CO photorelease with high efficiency. If the $^1T_1$ state of the model compounds employed here is at an energy comparable to that for carboxyhemoglobin,[10] then there are no singlet states at such low energies and the acceptor state must be of triplet (or higher) multiplicity. Since sensitized dissociation of Fe(Por)(CO) and generation of triplet Zn(Por) occur with comparable efficiencies, we conclude that the acceptor level is the porphyrin $^3(\pi \rightarrow \pi^*)$ level itself (Figure 7). This conclusion is supported by the observation that Fe(TPP)(CO) and the less sterically hindered Fe(DPD)(CO) are sensitized with comparable efficiency (F_m) and that the F_m for the several effective donors are all of comparable magnitude. It is possible that sensitized photodissociation actually occurs from $^3(\pi \rightarrow \pi^*)$ directly, in accordance with our earlier suggestion. As an alternative, one might propose that triplet transfer to $^3(\pi \rightarrow \pi^*)$ is followed by relaxation to lower lying ligand field states.

The present experiments of course do not necessarily show the pathway followed by energy directly absorbed by Fe(Por)(CO). However, they naturally suggest that photoexcitation to one of the allowed porphyrin-like $^1(\pi-\pi^*)$ levels is followed by internal conversion to the lowest such level, ^1Q, and by intersystem crossing to the $^3(\pi-\pi^*)$ level, ^3Q, without significant population of $^1T_1$. The actual dissociating state(s) could be the lowest lying ligand field excitations, which would be reached by further relaxation. For example, Chernoff et al.[31] now implicate the carboxyheme $^3T_1$ and $^5T_2$ states in the dissociation process. However, there is no direct evidence regarding this portion of the process, and the CO photorelease quantum yield is far higher than normally observed in cases where the dissociating state is a ligand field excitation.[29] This leads us to recall the suggestion[9] that ligand release might occur directly from $(\pi-\pi^*)$ configurations, for reasons noted above.

Acknowledgment. We thank Professor K. G. Spears, Dr. W. Euler, and Mr. S. Brugge for technical assistance. This work has been supported by the NSF (Grant PCM 768130X) and NIH (Grant HL 13531).

Appendix

The shape of the curves of $F(D)$ vs. $[D]$ can be reproduced through consideration of the reactions which occur during and after the photolysis flash. During a time-resolved sensitization measurement, donor D and acceptor Q undergo the processes shown in Scheme II. The concentrations of excited triplet donor, D*, and "excited" acceptor, Q*, are described by two coupled differential equations (A1) and (A2). These equations include

$$\frac{d[D^*]}{dt} = \omega_D I_D([D],t) - \bar{k}_1[D^*] - \bar{k}_2[D^*]^2 \qquad (A1)$$

$$\frac{d[Q^*]}{dt} = \omega_Q I_Q([D],t)[Q] + k_e[D^*][Q] - k_g[Q^*] \qquad (A2)$$

terms for direct photoexcitation and collective sums of first-order and second-order rate processes which affect D* and Fe populations in the sample. The parameters involved have the definitions given in (A3)–(A5) with definitions: k_{1g}, triplet ground quenching

$$\bar{k}_1 = k_{1g} + k_u + k_Q[Q_0] \qquad (A3)$$

$$\bar{k}_2 = k_{sq} - k_{1g} \qquad (A4)$$

$$I_\alpha([D],t) = I(t)\exp(-\epsilon_\alpha^D l[D]) \qquad (A5)$$

rate; k_u, triplet state unimolecular decay rate; k_q, second-order

(26) Caldwell, R. A.; Creed, D.; Maw, T.-S. *J. Am. Chem. Soc.* **1979**, *101*, 1293–1295.
(27) Balzani, V.; Bolletta, F.; Scandola, F. *J. Am. Chem. Soc.* **1980**, *102*, 380–399.
(28) Zerner, M.; Gouterman, M.; Kobayashi, H. *Theor. Chim. Acta* **1966**, *6*, 363–400.
(29) (a) Balzani, V.; Carassiti, V. "Photochemistry of Coordination Compounds"; Academic Press: New York, 1970. (b) Adamson, A. W.; Fleischauer, P. D. "Concepts of Inorganic Photochemistry"; Wiley-Interscience: New York, 1975.
(30) Kirchner, R. F.; Loew, G. H. *J. Am. Chem. Soc.* **1977**, *99*, 4639–4647.
(31) Chernoff, D. A.; Hochstrasser, R. M.; Steele, A. W. *Proc. Natl. Acad. Sci. U.S.A.* **1980**, *77*, 5606–5610.

rate constant for quenching of D* by k_{sq}, triplet self-quenching rate; k_e, rate constant for the process by which energy transfer from D* to Q results in Q* production; k_g, decay rate constant for Q*. The parameters ω_α, the extinction coefficients ϵ_α^D, and the distance l are discussed above. The photolysis pulse, with total duration τ, is assumed to have a time-dependent total flux, $I(t)$, incident on the cuvette face.

The triplet quenching rates, k_q, for Fe(Por)(py)(CO) and Fe(Por)$(py)_2$ are equal (see above), and in any case the fraction of excited acceptor molecules is normally small. Thus, the quenching term in eq A3 is written in terms of $[Q_0] = [Q] + [Q^*]$, the total concentration of acceptor. As a consequence, solution of eq A1 and A2 for all times is straightforward. Upon assumption of a functional form for $I(t)$, eq A1 may be integrated to obtain $[D^*](t)$, and this function then used for the solution of (A2).

As one example, with the assumption of a square pulse with flux I_0 for $0 \le t \le \tau$, the time during the interval (τ) in which the pulse persists, the general solution of (A1) is

$$[D^*_I](t) = U\left\{1 - e^{-(\tilde{k}_1+2\tilde{k}_2U)t}\left[\frac{\tilde{k}_1 + 2\tilde{k}_2U}{\tilde{k}_2 + \tilde{k}_2U(1 + e^{-(\tilde{k}_1+2\tilde{k}_2U)t})}\right]\right\} \quad (A6)$$

where $U = (1/2\tilde{k}_2)\{[\tilde{k}_1^2 + 4\tilde{k}_2\omega_D I_D(D)[D]]^{1/2} - \tilde{k}_1\}$ and $\tilde{k}_1 = \bar{k}_1 + I_0\omega_D$. The results from the triplet state quenching section can be used to estimate all the parameters in eq 6. Under the conditions of our experiment (total donor, $[D_0] \approx 10^{-4}$ M, $[Q_0] \approx 2 \times 10^{-6}$ M), we find that the first-order decay terms dominate eq A6 and, further, that $\tilde{k}_1 \approx \bar{k}_1 \approx k_q[Q_0]$. In this case the D* triplet population during photolysis follows the expression

$$[D^*_I](t) = \frac{\omega_D I_D(D)[D]}{\bar{k}_1}(1 - e^{-\bar{k}_1 t}) \quad t \le \tau \quad (A7)$$

For times $t > \tau$, whatever has been the flash profile, the donor triplet decays exponentially

$$[D^*_{II}](t) = [D^*](\tau)e^{-\bar{k}_1(t-\tau)} \quad t \ge \tau \quad (A8)$$

At any time, the total fraction of Q* produced, $f = [Q^*]/[Q_0]$, obeys eq A9 and in particular, for $t > \tau$, after the photolysis pulse,

$$\Omega([D],t) \equiv -\ln(1 - f) = \omega_Q\int_0^t I([D],t)\,dt + k_e\int_0^t [D^*](t)\,dt - k_g t \quad (A9)$$

the second term separates into two integrals, one over the time of the flash and the other for subsequent times.

$$\int_0^t [D^*](t)\,dt = \int_0^\tau [D^*_I](t)\,dt + \int_\tau^t [D^*_{II}](t)\,dt \quad (A9a)$$

A fully time-resolved sensitization experiment would involve observations at an arbitrary time, although typically for times $t > \tau$, and equations for such experiments will be presented later. In the present quasi-time-resolved experiments several limiting conditions have been imposed. First, over the time course of Q* creation ($t \lesssim 1/\bar{k}_1$), it is possible to adjust the pyridine and CO concentrations such that recombination (k_g) can be ignored. Second as noted just above, we are operating under low levels of donor excitation such that $\tilde{k}_1 \approx \bar{k}_1$ and $\bar{k}_2$ may be ignored. Finally, observations begin at times $t > 1/\bar{k}_1$ when all creation processes have ceased. Under these conditions, the fraction of Q* observed at the temporal origin in the fit to a Q* decay trace is precisely the total fraction of Q* produced by all processes. It is obtained from eq A9 by ignoring k_g and letting $t \to \infty$ in the integration (eq A9a). With the restrictions noted, it may be proved that the result is independent of the shape of the exciting pulse and is given by eq A10, where $J = \int_0^t I(t)\,dt$ and the effective quantum yield,

$$\Omega(D) = -\ln(1 - f) = \Gamma(D)J \quad (A10)$$

Γ, is given by eq A11. We note that linearity of a plot of Ω vs.

$$\Gamma(D) = \omega_Q e^{-\epsilon_Q^D l[D]} + \frac{k_e}{\bar{k}_1}\omega_D[D]e^{-\epsilon_D^D L[D]} \quad (A11)$$

J, in conformance with eq A10, provides a confirmation that the photon flux is sufficiently low such that $\tilde{k}_1 \approx \bar{k}_1$ and that second-order processes ($\bar{k}_2$) may be ignored, for otherwise such plots would be nonlinear. The results are typically discussed in terms of the ratio

$$F(D) = \frac{\Gamma(D)}{\Gamma(Q)} = e^{-\epsilon_Q^D l[D]} + \frac{k_e}{\bar{k}_1}\frac{\omega_D}{\omega_Q}De^{-\epsilon_D^D l[D]} \quad (A12)$$

If $\epsilon_Q^D = 0$, this may be rewritten as eq A13 and A14 with $\delta = [D]/[D_m^0] = (\epsilon_D^D l)^{-1}[D]$ and a maximum value of F at $\delta = 1$.

$$F^0(\delta) = 1 + A^0\delta e^{-\delta} \quad (A13)$$

$$A_0 = \frac{k_e}{\bar{k}_1}\frac{\omega_D}{\omega_Q}[D_m^0] \quad (A14)$$

If $\rho = \epsilon_Q^D/\epsilon_D^D > 0$ (partial overlap of D and Q absorptions), the maximum of Γ is shifted to lower concentration, $[D_m]$. Defining $\sigma = [D_m]/[D_m^0]$ and redefining $\delta = [D]/[D_m]$, then $F(\delta)$ becomes

$$F(\delta) = e^{-\rho\sigma\delta} + Ae^{-\sigma\delta} \quad (A15)$$

where A is now given by eq A14, but with the exception that the observed value $[D_m]$ replaces $[D_m^0]$. This allows us to express A and F_m in terms of σ and $\rho > 0$

$$A = \frac{\rho\sigma e^{-\sigma(\rho-1)}}{1 - \sigma} \quad (A16)$$

$$F_m = \left(1 + \frac{\rho\sigma}{1 - \sigma}\right)e^{-\sigma\rho} = e^{-\sigma\rho} + Ae^{-\sigma} \quad (A17)$$

Thus, since ρ is fixed by the absorption characteristics of Q and D and by the excitation source, a measured value of F_m uniquely specifies a value of σ and of the experimentally interesting parameter, A.

Incorporating the effects of donor light absorbance on the direct FeCO photodissociation through inclusion of a nonzero value for ρ significantly improves the correspondence between the predicted curve for F and that observed experimentally. For example, in no case studied does the estimated effective values for the ratio of porphyrin and donor reach 0.5, that is $\rho < 0.5$. Therefore, for comparison purposes we have presented in Figures 5 and 6 two curves, one calculated from eq A13 which assumes $\rho = 0$, the other from eq A15 with $\rho = 0.5$. For donor concentrations such that $\delta \le 1$, the curves for $\rho = 0$ and $\rho = 0.5$ have indistinguishable shapes. However, for $\delta > 1$ the inclusion of $\rho > 0$ marked sharpens the drop in F, even to values below unity. The improved correspondence between experiment and theory is clearly seen in the figures.